

Production of high-quality Pt single crystals using a new flame float-zone method

Nagakazu Furuya,* Masaki Ichinose and Masami Shibata

Department of Applied Chemistry, Faculty of Engineering, Yamanashi University, 4-3 Takeda, Kofu 400-8511, Japan. E-mail: furuya@ab11.yamanashi.ac.jp; Fax: +81 552 20 8560; Tel: +81 552 20 8559

Received 9th February 2001, Accepted 10th May 2001

First published as an Advance Article on the web 12th June 2001

Production of large and dislocation-free Pt single-crystal electrodes using a new flame float-zone (FFZ) method, of which the key technique is to use dislocation-free Pt for making a Pt single-crystal bead, is proposed. The qualities of the Pt single crystal using the FFZ method and a flame melting (FM) method, the so-called Clavilier's method, are compared using electrochemical measurements and AFM observations. To obtain wide, atomically flat terraces with monatomic steps at Pt(111) and Pt(100), the necessary annealing time for FFZ Pt single crystal and FM Pt single crystal was 180 min and > 180 min, respectively. The epitaxial rearrangement of surface atoms would be performed rapidly for the FFZ Pt single crystal. Moreover, the roughness of the FM Pt(111) and Pt(100) planes after etching was significantly greater than that of the FFZ Pt(111) and Pt(100) planes. Thus the surface structures of the Pt single crystal made using the FFZ method seem to be a more perfect crystal than those using the FM method. The FFZ Pt(100) facets for measurements of STM, AFM and IR are more desirable than the FM Pt(100) facets because the size of FFZ Pt(100) facets is larger than that of the FM(100) facets.

1. Introduction

In the last two decades of the 20th century, well-defined Pt single-crystal surfaces were obtained and studied by many electrochemists. These well-defined surfaces afforded us a powerful tool to approach the mystery of the hydrogen and oxygen peaks, as well as the structural effect in electrocatalysis, which has been studied extensively by many authors.^{1–60} It has been realized that several electrochemical reactions are strongly dependent on crystallographic orientations.

In the past decade, surface analysis techniques of scanning tunneling microscopy (STM) and *in-situ* infrared spectroscopy (IR) have been applied to investigations of atomic-level surface structure and adsorbed molecules at the solid–liquid interface.^{46–49,52–60} The facets on the Pt beads and the mechanically exposed planes post-treated with the so-called flame annealing and quenching method^{11,12} are widely used for STM and IR measurements. Therefore, a superior quality of Pt single-crystal electrode is required as the substrate.

The Pt single-crystal electrodes were usually made using the flame melting (FM) method, the so-called Clavilier's method.^{11,12} The mechanically exposed Pt single-crystal planes were annealed in a flame, quenched in water, and then exposed to the electrolyte. In this way, this method is a unique and convenient way to prepare a well-defined single crystal. However, it is difficult to make a large single crystal by the FM method.

In this paper, we propose the production of large and dislocation free Pt single crystals using the flame float-zone (FFZ) method. Moreover, the qualities of the platinum single crystal using the FM method and the FFZ method were evaluated and compared.

2. Experimental

2.1 Production of Pt single crystal

2.1.1 Flame float-zone method (FFZ method). The center of a Pt wire (diameter = 1 mm, 99.99% purity) was melted locally in an oxygen-rich hydrogen flame, as shown in Fig. 1(A). The melted float zone was moved gradually toward the end (y). A single crystal with high quality began to form at the cooling part of the melted float zone (b), being out of the flame, and then was grown at the center of the Pt wire, as shown in Fig. 1(B). This procedure is similar to Dash's technique⁶¹ for growing dislocation free silicon crystals. Part (c) of the Pt single crystal would be dislocation-free. In particular, there is likely to be no dislocation in the thinner part (d). Lattice defects and impurities in the melted float zone (b) of Pt would be concentrated in the part (e). Part (c) close to part (d) was then melted gradually toward (x). A large single crystal (g) was grown using part (d) as a seed and was separated from part (x) of the Pt wire by melting at part (h), as shown in Figs. 1(C), (D) and (E). A large single-crystal bead (i) was produced by melting and cooling carefully. The position of the Pt wire was horizontal as shown in Fig. 1(A) to (D), or vertical as shown in Fig. 1(E). In this paper, the FFZ Pt single crystal and FFZ Pt(*hkl*) represent Pt single crystals made using the FFZ method.

2.1.2 Flame melting method (FM method). The lower part of a Pt wire (diameter = 1 mm, 99.99% purity), held perpendicularly, was melted locally in an oxygen-rich hydrogen flame. The melted Pt bead was grown by bringing it close to the flame. By keeping the bead carefully away from the flame, the temperature of the platinum melt was lowered slowly, and

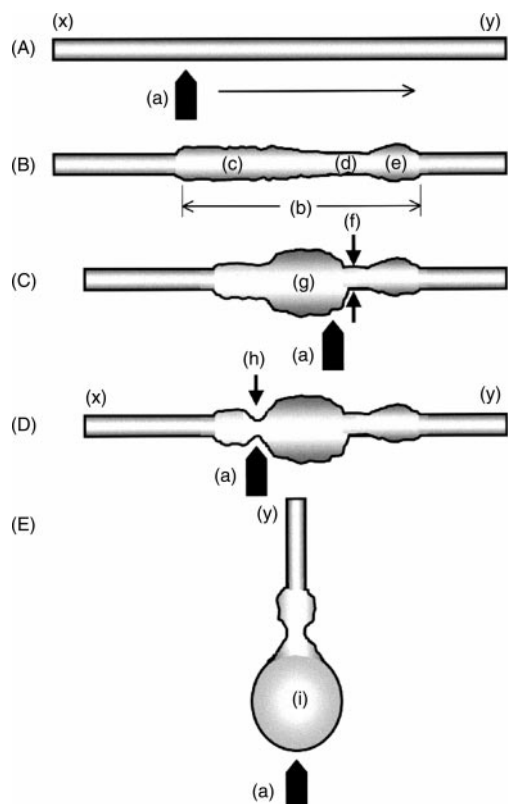


Fig. 1 Schematic diagrams (A)–(E) for procedure of the FFZ method. (x) and (y) Pt wire, (a) oxygen-rich hydrogen flame, (b) melting float zone, (c) and (d) dislocation-free single crystal, (e) Pt single crystal with trace amounts of dislocations and impurities, (f) seed crystal, (g) re-melting single crystal, (h) cutting by melting, (i) dislocation-free Pt single-crystal bead.

the Pt bead was made to recrystallize in 30 s. It can change to a polycrystal, when it crystallizes in a short time.

2.1.3 Orientation, cutting and polishing of single-crystal planes. The single crystal was oriented by the laser beam method and then cut to expose the Pt(111) and Pt(100) planes.^{11,12,18} Moreover, the surface of the exposed plane was lapped with diamond paste and polished with fine diamond paste. The surface was then annealed at 1773 K in a flame.¹⁹

2.2 Evaluation of single crystals

2.2.1 Electrochemical measurements. For electrochemical characterization of the Pt surface, the single crystal was annealed at 1773 K for 5 s, again in a flame, cooled immediately in a stream of helium gas with 0.1% hydrogen,¹⁸ and then immersed in ultra pure water saturated with hydrogen. The electrode mounted in its all-glass holder was transferred to an electrochemical cell,¹⁸ while protecting the single-crystal surface with a drop of water.¹¹ Measurements of the linear sweep voltammograms were conducted by the dipping method.¹¹ Sulfuric acid solution ($0.05 \text{ mol dm}^{-3} = 0.05 \text{ M}$) was prepared by dissolving reagent grade H_2SO_4 in twice-distilled water. All potentials were referenced to a reversible hydrogen electrode (RHE).

2.2.2 Observation of surface. For AFM observation in air, the single-crystal bead was annealed at 1773 K for 3 s again in a flame and was cooled in a stream of helium gas with 0.1% hydrogen.¹⁸ The facets and surface of the Pt single-crystal bead and the single-crystal planes prepared by cutting and polishing were observed using an optical microscope (OM) with a CCD camera (Shimadzu, CCD-F3000), a scanning electron microscope (SEM: JEOL, JSM-5310LV) and an atomic force microscope (AFM: SII, SPI-3800, SPA300).

3. Results and discussion

3.1 Observation of external appearance and cross section

The size of a single crystal made using the FFZ method was about 4 mm in diameter. The area of the FFZ Pt(111) and FFZ Pt(100) facets of the platinum single crystal were more than 2 and 0.25 mm^2 , respectively.

On the other hand, the size of the single crystal made using the FM method was about 3 mm in diameter. By careful preparation of FM Pt single crystal, it is possible to make a large bead.^{55–60} Generally, it is difficult to make such a large bead of a single crystal because a Pt single crystal made using the FM method has to grow from a microcrystal, as a seed, in Pt wire. Therefore, the prospects of making a Pt single crystal are no more than about 10%, that is, the greater part of such large Pt beads prepared using the FM method were Pt polycrystals. The area of the FM Pt(111) facets was less than 1.5 mm^2 . The Pt(100) facets seldom appeared for the Pt beads made using the FM method. The area of Pt(100) facets obtained occasionally was smaller than 0.04 mm^2 . STM and AFM measurements on the FM Pt(100) facet are more difficult than those on the FFZ Pt(100) facet because the FFZ Pt(100) facets are larger.

AFM observation was carried out on the facets of FFZ Pt(111) and FM Pt(111) etched for 30 min in aqua regia ($\text{HNO}_3 : \text{HCl} : \text{H}_2\text{O} = 1 : 10 : 5$). The terraces and steps at the facets of FFZ Pt(111) and FM Pt(111) disappeared after the etching. Many etch pits, which are considered crystal defects, were observed on the facets of FFZ Pt(111). There were approximately 10^9 crystal defects. No pits were observed on the facets of FM Pt(111) though the whole surface was etched to roughness. AFM observation was carried out on the facets of FFZ Pt(100) and FM Pt(100) etched for 30 min in aqua regia ($\text{HNO}_3 : \text{HCl} : \text{H}_2\text{O} = 1 : 10 : 5$). The terraces and steps at the facets of FFZ Pt(100) and FM Pt(100) disappeared after the etching. There were approximately 4×10^9 crystal defects on both facets of FFZ Pt(100) and FM Pt(100). There were few crystal defects on the facets of FFZ Pt and FM Pt single crystals.

A cross section of FFZ Pt and FM Pt single crystals was exposed by cutting and lopping, and then etching with aqua regia for 30 min. The cross section was observed using an optical microscope. Although grain boundaries were not observed on the surface of the FM Pt single crystal, there are a few grain boundaries in the body of the FM Pt single crystal. In the case of the FFZ Pt single crystal, there were no grain boundaries either on the surface or in the body. On melting and removing impurities in the Pt wire, the melted float zone [the part (b) in Fig. 1(B)] was crystallized gradually. As a result, parts (c) and (d) of the Pt single crystal became dislocation-free, and lattice defects and impurities in the melted float zone (b) of Pt were moved and concentrated into part (e).

3.2 AFM observation on Pt(111) and Pt(100) facets

The Pt(111) facets on the Pt beads made using the FFZ method and the FM method were observed with an AFM. Atomically flat terraces with monatomic steps were found at both Pt(111) facets.

The Pt(100) facets on the Pt beads made using the FFZ method and the FM method were observed with the AFM. Atomically flat terraces with monatomic steps were found at both Pt(100) facets. There were some square islands with monatomic steps,⁵² of which the sizes on FFZ Pt(100) and FM Pt(100) were about $50 \text{ nm} \times 50 \text{ nm}$ and about $15 \text{ nm} \times 15 \text{ nm}$, respectively, on the wide atomically flat terraces.

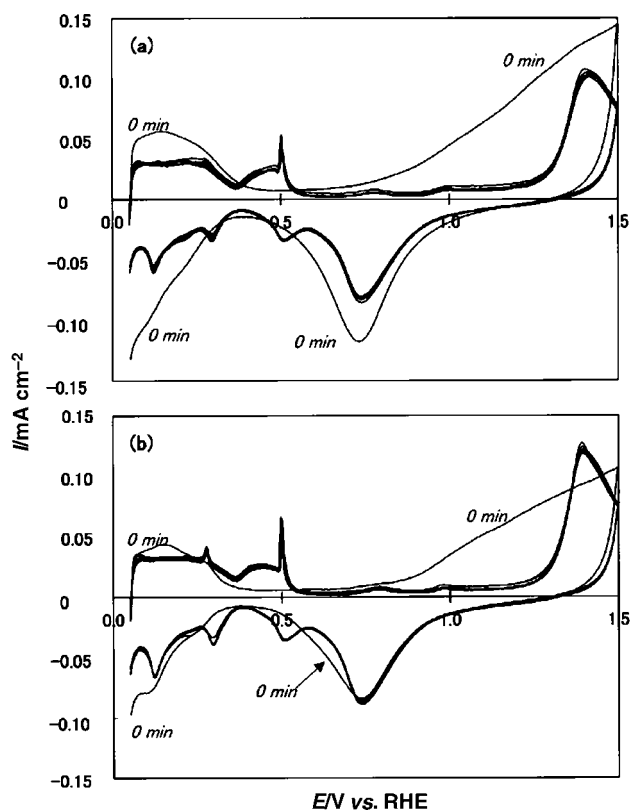


Fig. 2 Voltammograms (sweep rate: 0.05 V s^{-1}) for various annealing times at Pt(111) face in a $0.1 \text{ M H}_2\text{SO}_4$ solution. (a) FFZ method, (b) FM method.

3.3 Influence of surface structure at mirror-like polished Pt single crystal on annealing time

After a so-called “mirror-like” polish, Pt single-crystal electrodes were annealed for various times (from 1 min up to 180 min) at 1773 K in a gas–oxygen flame. After different annealing times, the CV measurements and AFM observations were carried out.

3.3.1 Voltammograms. The linear sweep voltammograms at the Pt(111) annealed for various times are shown in Figs. 2(a) and (b). The voltammograms at the Pt(111) without annealing were widely different from the well-known voltammogram^{1,18} of an atomically flat Pt(111), which was observed at the FFZ Pt(111) and FM Pt(111) annealed for >1 min. The voltammograms at the Pt(111) annealed for 5, 20, 40, 60, 120 and 180 min were similar. By careful preparation of FM Pt(111)^{56,58,60} it is possible to eliminate the small peak in Fig. 2(b).

The linear sweep voltammograms at the Pt(100) annealed

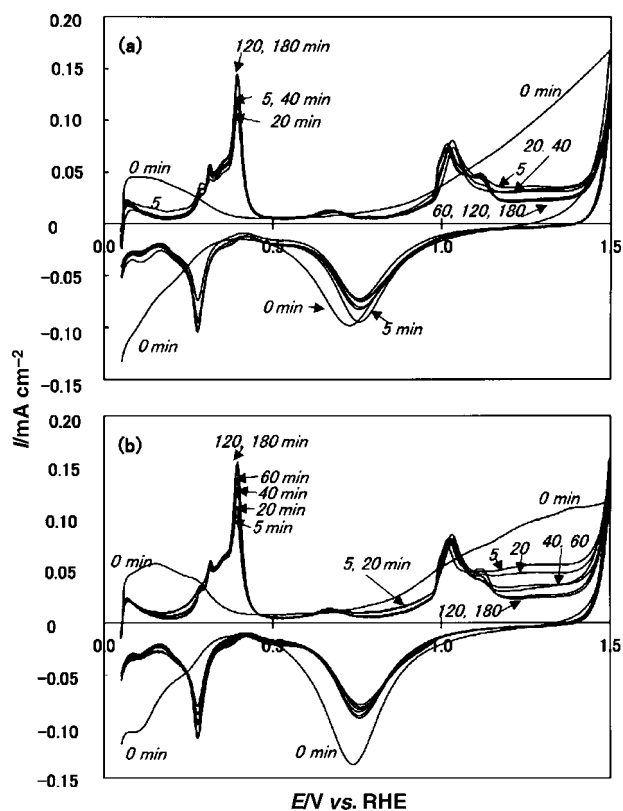


Fig. 3 Voltammograms (sweep rate: 0.05 V s^{-1}) for various annealing times at Pt(100) face in a $0.1 \text{ M H}_2\text{SO}_4$ solution. (a) FFZ method, (b) FM method.

for various times are shown in Figs. 3(a) and (b). The voltammograms at the Pt(100) without annealing were widely different from the well-known voltammogram^{49,50,52} of Pt(100) having atomically flat terraces. On increasing the annealing time, the anodic peak at 0.4 V becomes sharper and the currents from oxygen adsorption (at 1.1 V up to 1.5 V) decrease. The voltammograms at the potential range varied with the annealing time (0, 5, 20, 40, 60, 120 and 180 min).

The annealing time required for flatness after polishing of FFZ Pt(100) is shorter than that for FM Pt(100). The crystal structure in the FFZ Pt single crystal would be more perfect than that in the FM Pt single crystal. Therefore, rearrangement of the surface atoms on the FFZ Pt single crystal could be performed faster than those on the FM Pt single crystal.

3.3.2 AFM observation. AFM images on FFZ Pt(111) and FM Pt(111) after annealing for 1 min are shown in Figs. 4(a) and (b), respectively. Differences in height between a peak and a valley on each surface were about 20 nm and about 10 nm, respectively.

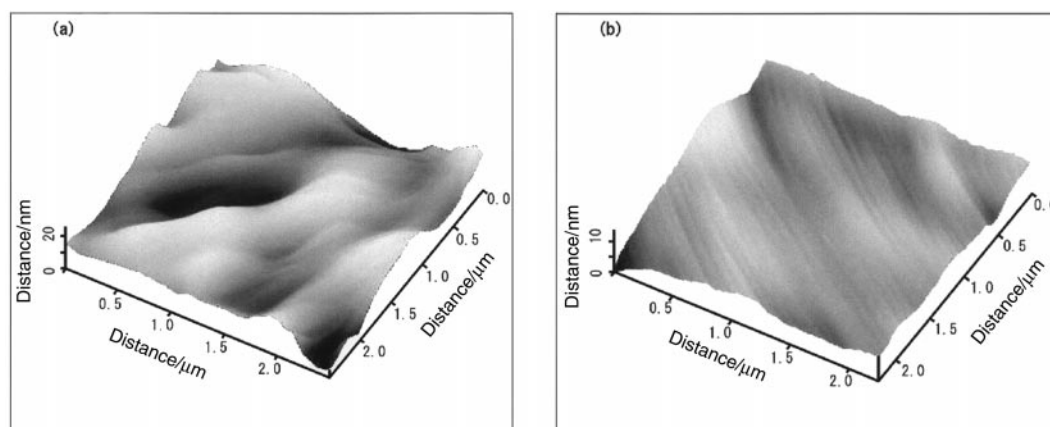


Fig. 4 AFM images of a Pt(111) face after annealing for 1 min. (a) FFZ method, (b) FM method.

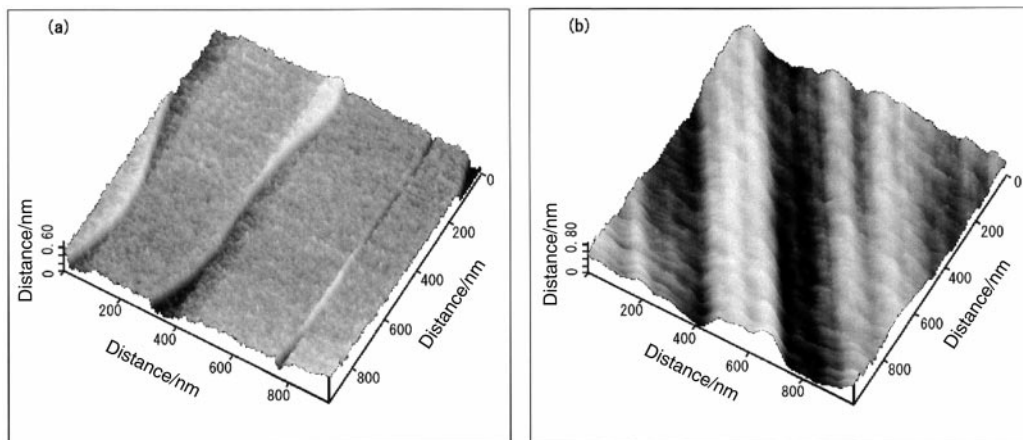


Fig. 5 AFM images of a Pt(111) face after annealing for 180 min. (a) FFZ method, (b) FM method.

AFM images on FFZ Pt(111) and FM Pt(111) after annealing for 180 min are shown in Figs. 5(a) and (b), respectively. The maximum difference in height on the image [Fig. 5(a)] of FFZ Pt(111) was approximately 0.6 nm. We found wide, atomically flat terraces with monatomic steps. The maximum

difference in height on the image [Fig. 5(b)] of FM Pt(111) was approximately 0.8 nm, corresponding to the height of three or four atoms. We did not find wide, atomically flat terraces with monatomic steps on the FM Pt(111) surface.

Typical AFM images on the FFZ Pt(100) and FM Pt(100)

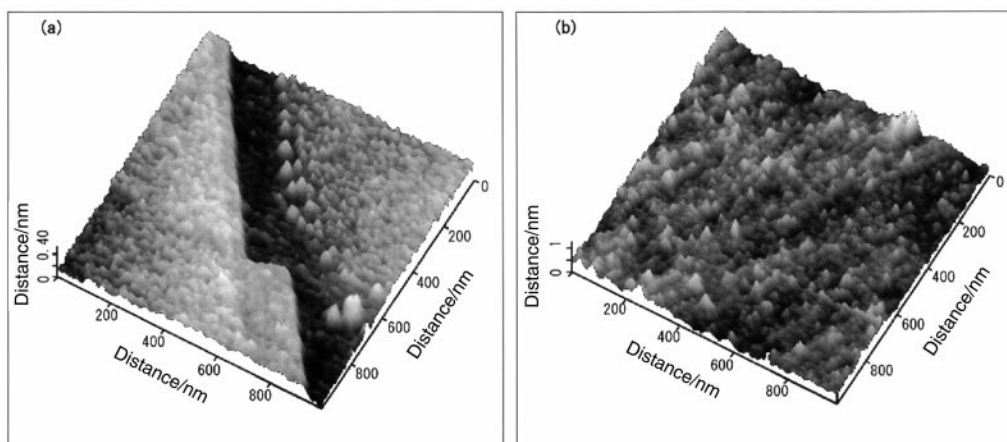


Fig. 6 AFM images of a Pt(100) face after annealing for 180 min. (a) FFZ method, (b) FM method.

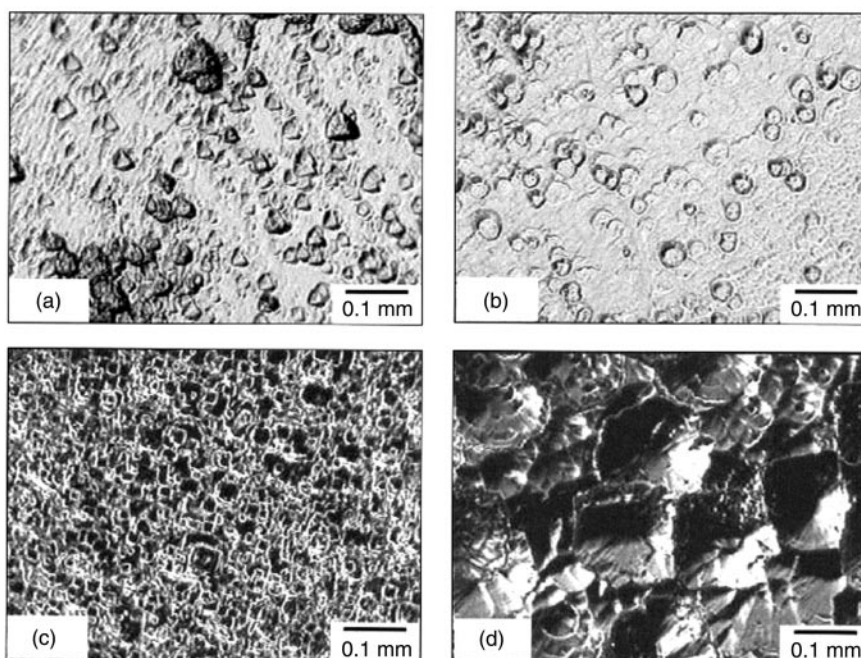


Fig. 7 Microphotographs of Pt(111) and Pt(100) faces after etching with aqua regia. (a) and (b) Pt(111), (c) and (d) Pt(100). (a) and (c) FFZ method, (b) and (d) FM method.

Table 1 Comparison of the size and surface structure between FFZ Pt and FM Pt facets

Sample	Size of facet/mm ²	Surface structure of facets
FFZ Pt(111)	2	Wide, atomically flat terrace with monatomic step
FM Pt(111)	1.5	Wide, atomically flat terrace with monatomic step
FFZ Pt(100)	0.25	Wide, atomically flat terrace
FM Pt(100)	0.04	Small flat terrace

Table 2 Comparison of quality between the well-defined FFZ Pt and the FM Pt planes

Method	Shape of etch pits on exposed plane after etching		Heat treatment time required for flatness after polishing/min	
	(111)	(100)	(111)	(100)
FFZ	Triangle	Small square	180	180
FM	Hexagon	Large square	>180	>180

after annealing for 180 min are shown in Figs. 6(a) and (b), respectively. The maximum difference in height on the image [Fig. 6(a)] of FFZ Pt(100) was approximately 0.4 nm. We found wide atomically flat terraces, where there were some small square islands⁵² with monatomic steps on FFZ Pt(100). We did not find wide, atomically flat terraces with monatomic steps on the FM Pt(100).

To obtain wide, atomically flat terraces with monatomic steps on Pt(111) and Pt(100), the necessary annealing time for FFZ Pt single crystal and FM Pt single crystal was 180 min and >180 min, respectively. The epitaxial rearrangement of surface atoms would be performed rapidly for the FFZ Pt single crystal, in which the atomic arrangement would be more perfect than for the FM Pt single crystal.

3.3.3 Surface of FFZ Pt and FM Pt single crystals after etching. Microscopic observation was carried out on the surface of FFZ Pt and FM Pt single crystals, which were annealed for 3 h after cutting and polishing and then etched for 30 min in aqua regia (HNO₃ : HCl : H₂O = 1 : 10 : 5). There are many etch pits on both surfaces of FFZ Pt(111) and FM Pt(111), as shown in Figs. 7(a) and (b). The shape of the etch pits on the FFZ Pt(111) was a regular triangle, while that on the FM Pt(111) appeared to be a circle or hexagon. The surface structure of the FFZ Pt(111) could be a more perfect crystal than that of the FM Pt(111).

Microphotographs were observed on FFZ Pt(100) and FM Pt(100) that were etched in aqua regia after cutting, polishing and annealing. Many etch pits, regular squares, appeared on both surfaces of FFZ Pt(100) and FM Pt(100), as shown in Figs. 7(c) and (d). The length of the regular squares at the FFZ Pt(100) and the FM Pt(100) was between 0.01 and 0.05 mm and approximately 0.1 mm, respectively. The roughness of the FM Pt(100) was significantly greater than that of the FFZ Pt(100). The surface structure of the FFZ Pt(100) would be a more perfect crystal than that of the FM Pt(100).

4. Conclusions

The results obtained in this work are summarized in Tables 1 and 2. The qualities of the Pt single crystal by the FFZ method and the FM method are compared.

The characteristics of FFZ Pt facets and FM Pt facets are compared in Table 1. The FFZ Pt(100) facets for measurements of STM, AFM and IR are more desirable than the FM Pt(100) facets because the size of FFZ Pt(100) facets is larger.

In Table 2, the qualities of the FFZ Pt(111), FFZ Pt(100), FM Pt(111) and FM Pt(100) exposed by cutting and polishing are summarized. The annealing time required for flatness after polishing of FFZ Pt(100) is shorter than that of FM Pt(100). The crystal structure of the FFZ Pt single crystal would be more perfect than that of the FM Pt single crystal. The rough-

ness of the FM Pt(111) and Pt(100) planes after etching was significantly greater than that of the FFZ Pt(111) and Pt(100) planes. Thus the surface structures on the FFZ Pt(111) and Pt(100) seem to be more perfect than those on the FM Pt(111) and Pt(100).

Although it is possible to make a large and good Pt bead by careful preparation of FM Pt single crystal,^{55–60} it is clear that the FFZ technique is an alternative and reliable way to the preparation of good Pt single crystals.

References

- 1 K. Yamamoto, D. M. Kolb, R. Kotz and G. Lehmppuhl, *J. Electroanal. Chem.*, 1979, **96**, 133.
- 2 K. Al Jaaf-Goize, D. M. Kolb and D. Scherson, *J. Electroanal. Chem.*, 1986, **200**, 353.
- 3 P. N. Ross, Jr., *J. Electroanal. Chem.*, 1977, **76**, 139.
- 4 F. T. Wagner and P. N. Ross, Jr., *J. Electroanal. Chem.*, 1983, **150**, 141.
- 5 P. N. Ross, Jr., *J. Electrochem. Soc.*, 1978, **126**, 67.
- 6 A. T. Hubbard, *J. Electroanal. Chem.*, 1978, **86**, 273.
- 7 E. Yeager, W. E. O'Grady, M. Y. C. Woo and P. Hagenn, *J. Electrochem. Soc.*, 1978, **125**, 348.
- 8 A. S. Homa, E. Yeager and B. D. Cahan, *J. Electroanal. Chem.*, 1983, **150**, 181.
- 9 E. Yeager, *J. Electrochem. Soc.*, 1977, **124**, 1932.
- 10 R. R. Adzic, W. E. O'Grady and S. Srinivasan, *Surf. Sci.*, 1980, **94**, L191.
- 11 J. Clavilier, R. Faure, G. Guinet and R. Durand, *J. Electroanal. Chem.*, 1980, **107**, 205.
- 12 J. Clavilier, *J. Electroanal. Chem.*, 1980, **107**, 211.
- 13 C. L. Scortichini and C. N. Reilly, *J. Electroanal. Chem.*, 1982, **139**, 233.
- 14 C. L. Scortichini and C. N. Reilly, *J. Electroanal. Chem.*, 1982, **139**, 247.
- 15 C. L. Scortichini and C. N. Reilly, *J. Electroanal. Chem.*, 1982, **139**, 265.
- 16 F. E. Woodard, C. L. Scortichini and C. N. Reilly, *J. Electroanal. Chem.*, 1983, **151**, 109.
- 17 B. Love, K. Seto and J. Lipkowski, *J. Electroanal. Chem.*, 1986, **199**, 219.
- 18 S. Motoo and N. Furuya, *J. Electroanal. Chem.*, 1984, **172**, 339.
- 19 S. Motoo and N. Furuya, *Ber. Bunsen-Ges. Phys. Chem.*, 1987, **91**, 451.
- 20 N. Furuya and S. Koide, *Surf. Sci.*, 1989, **220**, 18.
- 21 R. R. Adzic, A. V. Tripkovic and W. E. O'Grady, *Nature*, 1982, **296**, 137.
- 22 R. R. Adzic, A. V. Tripkovic and N. M. Markovic, *J. Electroanal. Chem.*, 1983, **150**, 79.
- 23 J. Clavilier, R. Durand, G. Guinet and R. Faure, *J. Electroanal. Chem.*, 1981, **127**, 281.
- 24 J. Clavilier, D. Armand and B. L. Wu, *J. Electroanal. Chem.*, 1982, **135**, 159.
- 25 J. Clavilier and D. Armand, *J. Electroanal. Chem.*, 1986, **199**, 187.
- 26 J. Clavilier, D. Armand and S. G. Sun, *J. Electroanal. Chem.*, 1986, **205**, 267.
- 27 D. Armand and J. Clavilier, *J. Electroanal. Chem.*, 1989, **263**, 109.
- 28 D. Armand and J. Clavilier, *J. Electroanal. Chem.*, 1989, **270**, 331.

- 29 J. Clavilier, K. El Achi and A. Rodes, *J. Electroanal. Chem.*, 1989, **272**, 253.
- 30 A. Rodes, K. El Achi, M. A. Zamakhchari and J. Clavilier, *J. Electroanal. Chem.*, 1990, **284**, 245.
- 31 A. Rodes, M. A. Zamakhchari, K. El Achi and J. Clavilier, *J. Electroanal. Chem.*, 1991, **305**, 115.
- 32 J. Clavilier, C. Lamy and J. M. Leger, *J. Electroanal. Chem.*, 1981, **125**, 249.
- 33 J. Clavilier, R. Parsons, R. Durand, C. Lamy and J. M. Leger, *J. Electroanal. Chem.*, 1981, **124**, 321.
- 34 C. Lamy, J. M. Leger, J. Clavilier and R. Parsons, *J. Electroanal. Chem.*, 1983, **150**, 71.
- 35 C. Lamy, J. M. Leger and J. Clavilier, *J. Electroanal. Chem.*, 1982, **135**, 321.
- 36 A. T. Hubbard, R. M. Ishikawa and J. Katekaru, *J. Electroanal. Chem.*, 1978, **86**, 271.
- 37 P. N. Ross, Jr., *J. Electrochem. Soc.*, 1979, **126**, 67.
- 38 S. G. Sung, J. Clavilier and A. Bewick, *J. Electroanal. Chem.*, 1988, **210**, 147.
- 39 J. Clavilier, A. Fernandez-Vega, J. M. Feliu and A. Aldaz, *J. Electroanal. Chem.*, 1989, **258**, 89.
- 40 A. Fernandez-Vega, J. M. Feliu, A. Aldaz and J. Clavilier, *J. Electroanal. Chem.*, 1989, **258**, 101.
- 41 J. Clavilier, A. Fernandez-Vega, J. M. Feliu and A. Aldaz, *J. Electroanal. Chem.*, 1989, **261**, 113.
- 42 S. Sun and J. Clavilier, *J. Electroanal. Chem.*, 1989, **263**, 109.
- 43 J. Clavilier, J. M. Orts, R. Gomez, J. M. Feliu and A. Aldaz, *J. Electroanal. Chem.*, 1996, **404**, 281.
- 44 R. R. Adzic, A. V. Tripkovic and W. O'Grady, *Nature*, 1982, **296**, 137.
- 45 S. Motoo and N. Furuya, *J. Electroanal. Chem.*, 1985, **184**, 303.
- 46 N. Kimizuka and K. Itaya, *Faraday Discuss.*, 1992, **94**, 117.
- 47 S. Tanaka, S.-L. Yau and K. Itaya, *J. Electroanal. Chem.*, 1995, **396**, 125.
- 48 Y.-G. Kim, S.-L. Yau and K. Itaya, *J. Am. Chem. Soc.*, 1996, **118**, 393.
- 49 M. S. Zei, N. Batina and D. M. Kolb, *Surf. Sci.*, 1994, **306**, 519.
- 50 J. Clavilier, J. M. Orts and J. M. Feliu, *J. Phys. IV*, 1994, **C1**, 303.
- 51 N. Kimizuka, T. Abe and K. Itaya, *Denki Kagaku*, 1993, **61**, 796.
- 52 N. Furuya, M. Ichinose and M. Shibata, *J. Electroanal. Chem.*, 1999, **460**, 251.
- 53 N. Furuya and M. Shibata, *J. Electroanal. Chem.*, 1999, **467**, 85.
- 54 N. Furuya, S. Motoo and K. Kunimatsu, *J. Electroanal. Chem.*, 1988, **239**, 347.
- 55 F. Huerta, E. Morallon, F. Cases, A. Rodes, J. L. Vazquez and A. Aldaz, *J. Electroanal. Chem.*, 1997, **421**, 179.
- 56 A. Rodes, J. M. Orts, J. M. Perez, J. M. Feliu and A. Aldaz, *J. Electroanal. Chem.*, 1997, **421**, 195.
- 57 F. Huerta, E. Morallon, F. Cases, A. Rodes, J. L. Vazquez and A. Aldaz, *J. Electroanal. Chem.*, 1997, **431**, 269.
- 58 J. M. Orts, A. Rodes and J. M. Feliu, *J. Electroanal. Chem.*, 1997, **434**, 121.
- 59 V. Climent, A. Rodes, J. M. Orts, J. M. Feliu and A. Aldaz, *J. Electroanal. Chem.*, 1997, **436**, 245.
- 60 V. Climent, A. Rodes, J. M. Orts, A. Aldaz and J. M. Feliu, *J. Electroanal. Chem.*, 1999, **461**, 65.
- 61 W. Dash, *J. Appl. Phys.*, 1958, **29**, 736.